SUNY-NTG-97-07

Strangeness production and flow in heavy-ion collisions

G. Q. Li[1,2], G. E. Brown[1], C.-H. Lee[1], and C. M. Ko[2]

[1] *Department of Physics, State University of New York at Stony Brook, Stony Brook, NY 11794*

[2] *Cyclotron Institute and Physics Department, Texas A&M University, College Station, Texas 77843*

Abstract

We study strangeness (K^+, K^-, and Λ) production and flow in Ni+Ni collisions at 1-2 AGeV, based on the relativistic transport model including the strangeness degrees of freedom. We find that strangeness spectra and flow are sensitive to the properties of strange hadrons in nuclear medium. The predictions of the chiral perturbation theory that the K^+ feels a weak repulsive potential and K^- feels a strong attractive potential are in good agreement with recent experimental data from FOPI and KaoS collaborations.

I. INTRODUCTION

With the development of various heavy-ion facilities, nuclear physics is expanding into many new directions. One of these is the study of the properties of strange particles, namely hyperons and kaons, in dense matter. Strangeness plays a special role in the development of hadronic and nuclear models. The mass of strange quark is about 150 MeV, which is, on the one hand, considerably larger than the mass of light (up and down) quarks (~ 5 MeV), but on the other hand, much smaller than that of charm quark (~ 1.5 GeV). In the limit of vanishing quark mass the chiral symmetry is good, and systematic studies can be carried out using chiral perturbation theory for hadrons made of light quarks. On the other hand, if

the quark mass is large, one can use the non-relativistic quark model to study the properties of charmed and heavier hadrons. The hadrons with strangeness lie in between these two limits and therefore present a challenge to the theorists.

Nevertheless, chiral perturbation calculations have been extensively and quite successfully carried out in the recent past for the study of kaon-nucleon (KN) and antikaon-nucleon ($\bar{K}N$) scattering [1,2]. The main reason for the success of the chiral perturbation theory is the existence of a large body of experimental data that can used to constrain the various parameters in the chiral Lagrangian.

Of great interest to nuclear physicists is the study of the properties of strange hadrons in dense matter. Chiral perturbation calculations in matter are still under development, since a new energy scale, the Fermi momentum, is now involved. For this kind of theoretical development to be successful, a large body of experimental data that can be obtained only from heavy-ion collisions are needed. The study of kaon properties in dense matter is also relevant for astrophysics problems, such as the properties of neutron stars [3].

There have been some studies on strangeness production and flow in heavy-ion collisions at SIS energies [4–10]. In this contribution we will concentrate on recent development concerning strangeness production in Ni+Ni collisions at 1-2 AGeV. We will show that these observables are sensitive to kaon properties in dense matter and can thus provide useful information for the development of chiral perturbation theory in matter and for the study of neutron star properties. In Section II, we review briefly the current understanding of kaon properties in nuclear matter, the relativistic transport model with strangeness, and the various elementary processes for strangeness production. Our results for strangeness spectra and flow will be reported in Section III, where we will also compare our results for proton and pion spectra to experimental data. Finally a brief summary is given in Section IV.

II. THE RELATIVISTIC TRANSPORT MODEL WITH STRANGENESS

Our study is based on the relativistic transport model extended to include the strange degrees of freedom [11]. The Lagrangian we use is given by

$$\begin{aligned}\mathcal{L} &= \bar{N}(i\gamma^\mu\partial_\mu - m_N + g_\sigma\sigma)N - g_\omega\bar{N}\gamma^\mu N\omega_\mu + \mathcal{L}_0(\sigma,\omega_\mu) \\ &+ \bar{Y}(i\gamma^\mu\partial_\mu - m_Y + (2/3)g_\sigma\sigma)Y - (2/3)g_\omega\bar{Y}\gamma^\mu Y\omega_\mu \\ &+ \partial^\mu\bar{K}\partial_\mu K - (m_K^2 - \frac{\Sigma_{KN}}{f^2}\bar{N}N)\bar{K}K - \frac{3i}{8f^2}\bar{N}\gamma^0 N\bar{K}\overset{\leftrightarrow}{\partial}_t K. \end{aligned} \quad (1)$$

In the above the first line gives the usual non-linear σ-ω model with the self-interaction of the scalar field. The second line is for the hyperons which couple to the scalar and vector fields with 2/3 of the nucleon strength, as in the constituent quark model. The last line is for the kaon which is derived from the SU(3) chiral Lagrangian. Note that since the hyperon and kaon densities in heavy-ion collisions at SIS energies are very small, their contributions to the scalar and vector fields are neglected.

From this Lagrangian we get the kaon and antikaon in-medium energies

$$\omega_K = \left[m_K^2 + \mathbf{k}^2 - a_K\rho_S + (b_K\rho_N)^2\right]^{1/2} + b_K\rho_N \quad (2)$$

$$\omega_{\bar{K}} = \left[m_K^2 + \mathbf{k}^2 - a_{\bar{K}}\rho_S + (b_K\rho_N)^2\right]^{1/2} - b_K\rho_N \quad (3)$$

where $b_K = 3/(8f_\pi^2) \approx 0.333$ GeVfm^3, a_K and $a_{\bar{K}}$ are two parameters that determine the strength of attractive scalar potential for kaon and antikaon, respectively. If one considers only the Kaplan-Nelson term, then $a_K = a_{\bar{K}} = \Sigma_{KN}/f_\pi^2$. In the same order, there is also the range term which acts differently on kaon and antikaon, and leads to different scalar attractions. We take the point of view that they can be treated as free parameters and try to constrain them from the experimental observables in heavy-ion collisions.

In chiral perturbation theory, in the same order as the Kaplan-Nelson term there is the range term, which can be taken into account by renormalizing [1]

$$\Sigma_{KN} \longrightarrow (1 - 0.37\frac{\omega_{K,\bar{K}}^2}{m_K^2})\Sigma_{KN}. \quad (4)$$

Since $\omega_K \sim m_K$ for the densitis considered here, there is a reduction of ~ 0.63 from the range term. However, f_π is also density dependent [12],

$$\frac{f_\pi^{*2}(\rho_0)}{f_\pi^2} \approx 0.6. \tag{5}$$

We do not know quantitatively the behaviour of f_π^*/f_π at higher densities, although we would expect it to continue to decrease with density. We see that, at least in the range of densities $\rho \sim \rho_0$, there is considerable cancellation between effects of the range term and the decrease in f_π. We therefore neglect both for K^+.

In the case of K^- meson, the range term drops rapidly with density as $(\omega_{\bar{K}}/m_K)^2$ decreases. We thus neglect the range term and relate $a_{\bar{K}}$ to a_K, namely, $a_{\bar{K}} \approx (0.63)^{-1} a_K$. Note that f_π^2 in b_K is not scaled with density. The b_K represents the vector interaction, which is 1/3 of the vector mean field acting on a nucleon. In our recent paper [13], it is shown that for $\rho \sim (2-3)\rho_0$, the region of densities important for kaon and antikaon production and flow, the nucleon vector mean field is estimated to be only about 15% larger than $3b_K = 9/(8f_\pi^2)$. The increase from scaling f_π^{-2} is evidently largely canceled by the decrease from short-range correlations. Our parameterization thus incorporates roughly what we know about the scaling of f_π and of effects from short-range interactions.

Using $a_K = 0.22$ GeV^{2}fm^3 and $a_{\bar{K}} = 0.35$ GeV^{2}fm^3, the kaon and antikaon effective mass, defined as their energies at zero momentum, are shown in Fig. 1. It is seen that the kaon mass increases slightly with density, resulting from near cancellation of the attractive scalar and repulsive vector potential. The mass of antikaon drops substantially. At normal nuclear matter density $\rho_0 \approx 0.16$ fm^{-3}, the kaon mass increases about 4%, in rough agreement with the prediction of impulse approximation based on KN scattering length. The antikaon mass drops by about 22%, which is somewhat smaller than what has been inferred from the kaonic atom data [14], namely, an attractive K^- potential of 200 ± 20 MeV at ρ_0.

From Fig. 1 we find that $m_{\bar{K}}(3\rho_0) \approx 170$ MeV. The correction for neutron rich matetr in using $m_{\bar{K}}$ in neutron stars is about 50 MeV upwards, giving $m_{\bar{K}}^* \approx 220$ MeV [15]. With the electron chemical potential of $\mu_e(3\rho_0) = 214$ MeV [16], this implies that kaon condensation

will take place at dnsity $\rho \sim \rho_0$.

From the Lagrangian we can also derive equations of motion for nucleons [8]

$$\frac{d\mathbf{x}}{dt} = \frac{\mathbf{p}^*}{\sqrt{\mathbf{p}^{*2} + m_N^{*2}}}, \quad \frac{d\mathbf{p}}{dt} = -\nabla_x(\sqrt{\mathbf{p}^{*2} + m_N^{*2}} + U_V), \tag{6}$$

for hyperons

$$\frac{d\mathbf{x}}{dt} = \frac{\mathbf{p}^*}{\sqrt{\mathbf{p}^{*2} + m_Y^{*2}}}, \quad \frac{d\mathbf{p}}{dt} = -\nabla_x(\sqrt{\mathbf{p}^{*2} + m_Y^{*2}} + (2/3)U_V), \tag{7}$$

and for kaons

$$\frac{d\mathbf{x}}{dt} = \frac{\mathbf{p}^*}{\omega_{K,\bar{K}} \mp b_k \rho_N}, \quad \frac{d\mathbf{p}}{dt} = -\nabla_x \omega_{K,\bar{K}}, \tag{8}$$

where $m_N^* = m_N - U_S$ and $m_Y^* = m_Y - (2/3)U_S$, with U_S and U_V being nucleon scalar and vector potentials. The minus and the plus sign in the last equation correspond to kaon and antikaon, respectively.

In addition to propagations in their mean field potentials, we include typical two-body scattering processes such as $BB \leftrightarrow BB$, $NN \leftrightarrow N\Delta$ and $\Delta \leftrightarrow N\pi$. Kaons and hyperons are mainly produced from the following baryon-baryon and pion-nucleon collisions, namely $BB \rightarrow BYK$, $\pi N \rightarrow YK$. The cross section for the former is taken to be the Randrup-Ko parameterization [17], and the cross section for the latter is taken from Cugnon *et al.* [18]. The antikaon production cross section in baryon-baryon collisions is taken from the recent work of Sibirtsev *et al.* [19], while that in pion-nucleon collisions is fitted to experimental data. Antikaons can also be produced from hyperon-pion collisons through the strangeness exchange process, namely, $\pi Y \rightarrow \bar{K}N$. The cross section for this process is obtained from the reverse one, $\bar{K}N \rightarrow \pi Y$, by the detailed-balance relation. The latter cross section, together with the $\bar{K}N$ elastic and absorption cross sections, are parameterized based on the available experimental data. We note that the antikaon absorption cross section is relatively large, and increases significantly with descreasing antikaon momentum, while kaons and hyperons undergo mainly elastic scattering with nucleons.

III. RESULTS AND DISCUSSIONS

We have studied strangeness production and flow mainly for Ni+Ni collisions at 1-2 GeV/nucleon. Our results for proton and pion transverse mass spectra in central Ni+Ni collisions at 1.06 AGeV are shown in Fig. 2. We determine our centrality to be $b \leq 2$ fm in order to compare with the FOPI data [20] which correspond to a geometric cross section of 100 mb. To get free protons we applied a density cut of $\rho \leq 0.15\rho_0$. It is seen that our model describes both the proton and pion spectra very well.

In the left panel of Fig. 3 we show our results for K^+ kinetic energy spectra in Ni+Ni collisions at 1.0 AGeV, with impact parameter $b \leq 8$ fm. The solid histogram gives the results with kaon medium effects, while the dotted histogram is the results without kaon medium effects. The open circles are the experimental data from the KaoS collaboration [21]. It is seen that the results with kaon medium effects are in good agreement with the data, while those without kaon medium effects slightly overestimate the data. We note that kaon feels a slightly repulsive potential, thus the inclusion of the kaon medium effects reduces the kaon yield. The slopes of the kaon spectra in the two cases also differ. With a repulsive potential, kaons are accelerated during the propagation, leading to a larger slope parameter as compared to the case without kaon medium effects.

The results for K^- kinetic energy spectra in Ni+Ni collisions at 1.8 AGeV are shown in the right panel of Fig. 3. The solid and dotted histograms are the results with and without kaon medium effects. It is seen that without medium effects, our results are about a factor 3-4 below the experimental data. With the inclusion of the medium effects which reduces the antikaon production threshold, K^- yield increases by about a factor of 3 and our results are in good agreement with the data. This is similar to the findings of Cassing *et al.* [10].

The KaoS data show that the K^- yield at 1.8 AGeV agrees roughly with the K^+ yield at 1.0 AGeV. This is a nontrial observation. At these energies, the Q-values for $NN \to NK\Lambda$ and $NN \to NNK\bar{K}$ are both -230 MeV. Near their thresholds, the cross section for the K^- production is about one order of magnitude smaller than that for K^+ production.

In addition, antikaons are strongly absorbed in heavy-ion collisions, which should further reduces the K^- yield. The KaoS results of $K^-/K^+ \sim 1$ indicate thus the importance of secondary processes such as $\pi Y \to \bar{K} N$ [22], and medium effects which acts oppositely on the kaon and antikaon production in medium.

In addition to particle yield, the collective flow of particles provide complimentary information about hadron properties in dense matter. In the left panel of Fig. 4 we compare our results for proton flow in Ni+Ni collisions at 1.93 AGeV with the experimental data from the FOPI collaboration [20]. Note that both the data and our results include a transverse momentum cut of $p_t/m > 0.5$. The agreement with the data is very good. The Λ flow in the same system is shown in the right panel of Fig. 4. The flow of the primodial Λ's, as shown in the figure by short-dashed curve, is considerably smaller than that of protons shown by dotted curve. Inclusions of ΛN rescattering (long-dashed curve) and propagation in potential (solid curve) increase the Λ flow in the direction of proton flow. Both the FOPI [20] and the EOS [23] collaborations found that the Λ flow is very similar to that of protons.

In the left panel of Fig. 5 we show our results for K^+ flow in Ni+Ni collisions at 1.93 AGeV, based on three scenarios for kaon potentials in nuclear medium. Without potential, kaons flow in the direction of nucleon as shown by the dotted curve. Without scalar potential, kaons feel a strong repulsive potential, and they flow in the opposite direction to nucleons as shown by the dashed curve. With both the scalar and vector potentials, kaons feel a weak repulsive potential, and one sees the disappearance of kaon flow, which is in good agreement with the experimental data from the FOPI collaboration [20]. In the right panel of Fig. 5 we show K^- flow in Ni+Ni collsions at 1.93 AGeV and $b = 4$ fm. Without medium effects one sees a clear antikaon antiflow signal, because of strong absorption of K^- by nucleons. Including the attractive antikaon potential, those antikaons that survive the absorption are pulled towards nucleon and thus show a weak antikaon flow signal. The experimental measurement of K^- in heavy-ion collisions will be very helpful in determining K^- properties in nuclear matter.

IV. SUMMARY

In summary, we studied strangeness (K^+, K^-, and Λ) production and flow in Ni+Ni collisions at 1-2 AGeV. We based our study on the relativistic transport model including the strangeness degrees of freedom. We found that strangeness spectra and flow are sensitive to the properties of strange hadrons in nuclear medium. The predictions of the chiral perturbation theory that the K^+ feels a weak repulsive potential and K^- feels a strong attractive potential are in good agreement with recent experimental data from FOPI and KaoS collaborations.

The work of GQL, GEB and CHL were supported in part by Department of Energy under Grant No. DE-FG02-88ER40388, while that of CMK was supported in part by the National Science Foundation under Grant No. PHY-9509266. CHL was also partly supported by Korea Science and Engineering Foundation.

REFERENCES

[1] C.-H. Lee, Kaon condensation in dense stellar matter, *Phys. Rep* 275:255 (1996).

[2] N. Kaiser, T. Waas, and W. W.Weise, Low energy $\bar{K}N$ interaction in nuclear matter, *Phys. Lett.* B365:12 (1996)

[3] R. Knorren, M. Prakash, and P. J. Ellis, Strangeness in hadronic stellar matter, *Phys. Rev* C52:3470 (1995)

[4] X. S. Fang, C. M. Ko, G. Q. Li, and Y. M. Zheng, The relativistic transport model description of subthreshold kaon production in heavy-ion collisions, *Nucl. Phys* A575:766 (1994)

[5] T. Maruyama, W. Cassing, U. Mosel, S. Teis, and K. Weber, Study of high-energy heavy-ion collisions in a relativistic BUU approach with momentum dependent mean fields *Nucl. Phys.* A573:653 (1994)

[6] C. Hartnack, J. Jänicke, L. Sehn, H. Stöcker, and J. Aichelin, Kaon production at subthreshold energies, *Nucl. Phys.* A580:643 (1994)

[7] G. Q. Li, C. M. Ko, and B. A. Li, Kaon flow as a probe of kaon potential in nuclear medium, *Phys. Rev. Lett.* 74:235 (1995)

[8] G. Q. Li and C. M. Ko, Kaon flow in heavy-ion collisions, *Nucl. Phys.* A594:460 (1995)

[9] G. Q. Li, C. M. Ko, and X. S. Fang, Subthreshold antikaon production in heavy-ion collisions, *Phys. Lett.* B329:149 (1994)

[10] W. Cassing, E. L. Bratkovskaya, U. Mosel, S. Teis, and A. Sibirtsev, Kaon versus antikaon production at SIS energies, *Nucl. Phys.*, to be published.

[11] C. M. Ko and G. Q. Li, Medium effects in heavy-ion collisions, *J. Phys.* G22:1673 (1996)

[12] G. E. Brown and M. Rho, From chiral mean field to Walecka mean field and kaon condensation, *Nucl. Phys.* A596:503 (1996).

[13] G. Q. Li, G. E. Brown, C.-H. Lee, and C. M. Ko, Nucleon flow and dilepton production in heavy-ion collisions, to be published.

[14] E. Friedman, A. Gal, and C. J. Batty, Density dependent K^- nuclear optical potential from kaonic atoms, *Nucl. Phys.* A579:518 (1994).

[15] G. E. Brown, Proc. Royal Dutch Academy Colloquium 'Pulsar Timing, General Relativity and the Internal Structure of Neutron Stars'. to be published

[16] V. Thorsson, M. Prakash, and J. M. Lattimer, Composition, structure and evolution of neutron stars with kaon condensation, *Nucl. Phys.* A572:693 (1994).

[17] J. Randrup and C. M. Ko, Kaon production in relativistic collisions, *Nucl. Phys.* A343: 519 (1980)

[18] J. Cugnon and R. M. Lombard, K^+ production in a cascade model for high-energy nucleus-nucleus collisions, *Nucl. Phys.* A422:635 (1984)

[19] A. Sibirtsev, W. Cassing, and C. M. Ko, Antikaon production in nucleon-nucleon reactions near threshold, *Z. Phys.* A, to be published.

[20] N. Herrmann, FOPI collaboration, Particle production and flow at SIS energies, *Nucl. Phys.* A610:49c (1996)

[21] P. Senger for the KaoS collaboration, kaon production in hadronic matter, *Heavy Ion Physics* 4:317 (1996)

[22] C. M. Ko, Subthreshold K^- production in high energy heavy-ion collisions, *Phys. Lett.* B120:294 (1983).

[23] M. Justice, EOS collaboration, Observation of collective effects in Λ production at 2 GeV/nucleon, *Nucl. Phys.* A590:549c (1995).

99

FIGURES

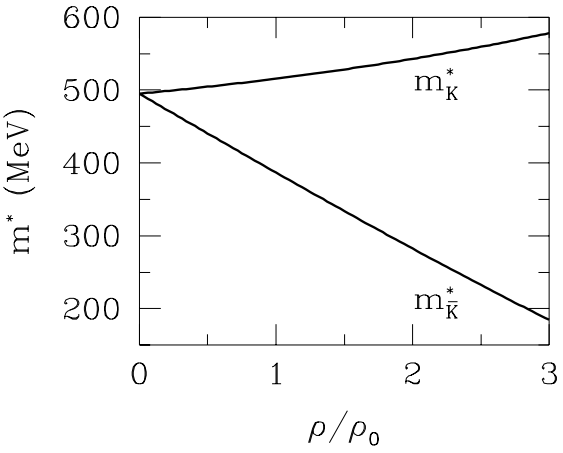

FIG. 1. Kaon and antikaon effective mass as a function of nuclear density

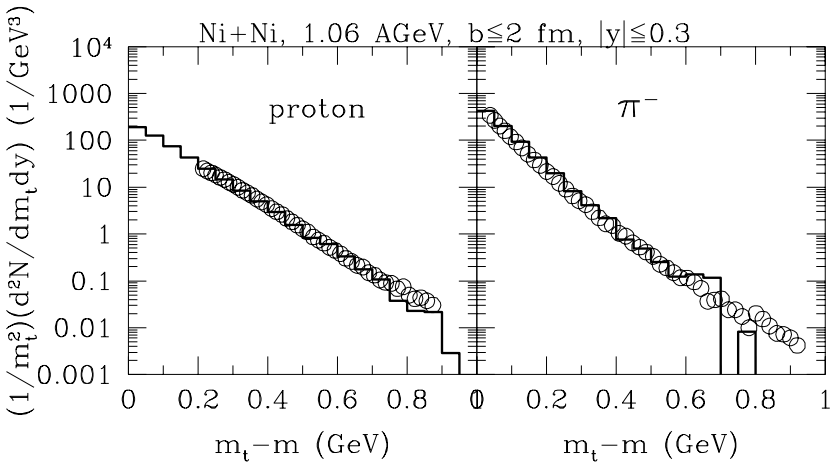

FIG. 2. Proton and pion transverse momentum spectra in central Ni+Ni collisions at 1.06 AGeV. The open circles are experimental data from the FOPI collaboration

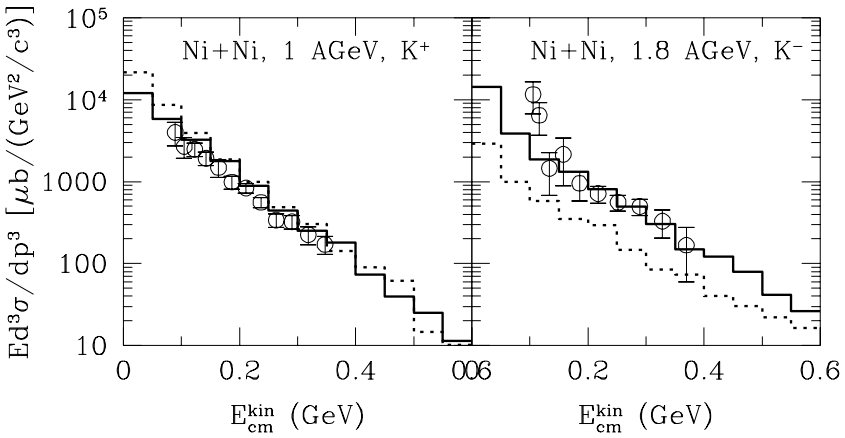

FIG. 3. Left panel: K^+ kinetic energy spectra in Ni+Ni collsions at 1.0 AGeV. Right panel: K^- kinetic energy spectra in Ni+Ni collisions at 1.8 AGeV. The solid and dotted histograms are the results with and without kaon medium effects. The open circles are the experimental data from the KaoS collaboration.

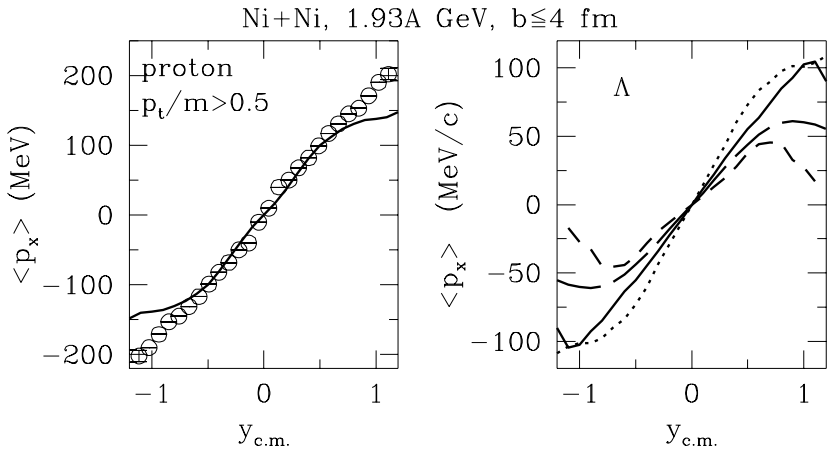

FIG. 4. Left panel: Proton flow in Ni+Ni collisons at 1.93 AGeV and $b \leq 4$ fm, including a transverse momentum cut of $p_t/m > 0.5$. The open circles are the experimental data from the FOPI collaboration. Right panel: Λ flow. The short-dashed curve is for primordial Λ's, the long-dashed curve includes elastic ΛN scattering, and the solid curve include both rescattering and propagation. The proton flow is shown by the dotted curve for comparison.

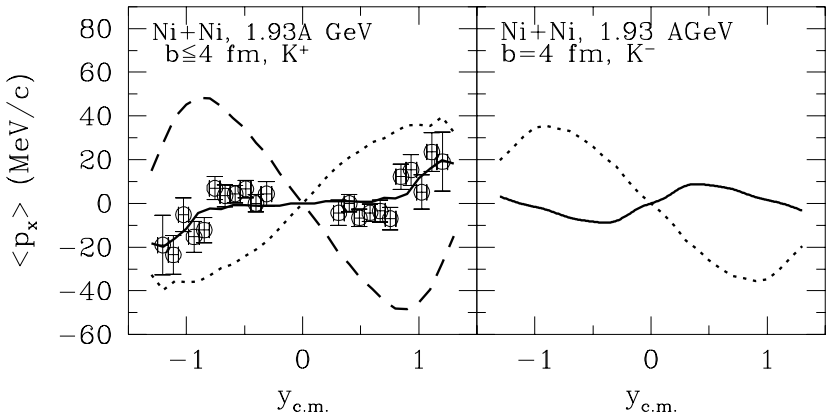

FIG. 5. Left panel: K^+ flow in Ni+Ni colliisons at 1.93 AGeV and $b \leq 4$ fm, including a transverse momentum cut of $p_t/m > 0.5$. The open circles are the experimental data from the FOPI collaboration. The dotted curve is the results without kaon potential, the dashed curve is the results without kaon scalar potential, and the solid curve gives the results with both the scalar and vector potential. Right panel: K^- flow in Ni+Ni collisions at 1.93 AGeV and $b = 4$ fm. The solid and dashed curves are the results with and without antikaon medium effects.